Polymer Journal (2012) 44, 278–285

www.nature.com/pj

ORIGINAL ARTICLE

Emission properties of cyclodextrin dimers linked with perylene diimide—effect of cyclodextrin tumbling

Yoshinori Takashima, Yu Fukui, Miyuki Otsubo, Norio Hamada, Hiroyasu Yamaguchi, Hitoshi Yamamoto and Akira Harada

Perylene diimide (PDI) derivatives with cyclodextrins (PDI-CD_2s) exhibit specific emission properties, which depend on the type of CDs in an aqueous solution. Herein we successfully create an emission film-kneaded PDI-CD_2 derivatives via effective tumbling of the altropyranose unit. PDI-6CD_2s are crosslinked with PDI between 6-amino-CDs. Although the emission intensities of PDI-6CD_2s in dimethyl sulfoxide are similar regardless of the type of CD, PDI-6γCD_2 has a relatively high emission intensity in aqueous solutions. In contrast, for PDIC_7-3CD_2s, which are linked with *N,N'*-bis(6-carboxylhexyl)perylene-3,4,9,10-tetracarboxyl diimide (BisC_7-PDI) between 3-amino-CDs, the emission intensity of PDIC_7-3βCD_2 is stronger than those of PDIC_7-3αCD_2, PDIC_7-3γCD_2, and PDI-6CD_2s in aqueous solutions. The selective emission behavior of PDIC_7-3CD_2s is due to the formation of the *pseudo*[1]rotaxane dimer through tumbling of the altropyranose unit in an aqueous solution. PDIC_7-3βCD_2 in the solid state does not demonstrate a distinctive emission due to self-quenching, whereas PDIC_7-3βCD_2 kneaded into the polyvinyl alcohol (PVA) film exhibits a bright yellow emission. The order of the emission intensities of PDIC_7-3CD_2s kneaded into PVA films is similar to those in aqueous solutions.
Polymer Journal (2012) **44**, 278–285; doi:10.1038/pj.2011.128; published online 18 January 2012

Keywords: cyclodextrins; fluorescence property; inclusion complex; perylene diimide; tumbling

INTRODUCTION

Recently, supramolecular assemblies with extended aromatic compounds have attracted much attention.[1–4] Perylene diimides (PDIs) derivatives effectively form supramolecular assemblies through π–π stacking interaction.[5–21] In particular, supramolecular assemblies based on calixarenePDI conjugates show efficient energy and electron transfer properties due to the well-defined rigid and electron-rich scaffolds of calixarenes.[22–27] We have prepared PDI derivatives with a high emission property in aqueous solutions.

Generally, PDI derivatives have low solubilities in aqueous solutions. Even if PDI derivatives are dissolved in aqueous solutions by introducing a hydrophilic group, the emission of PDI derivatives exhibit self-quenching in aqueous solutions due to the formation of supramolecular assemblies and folders. To create water-soluble and effective emission sensor materials with PDI derivatives, we have introduced CDs into the PDI motif. The CDs are a family of macrocyclic oligosaccharides; the most common are composed of 6 (α), 7 (β), or 8 (γ) α-1,4-linked D-glucopyranose units.[28–34] The introduction of CDs should influence the molecular recognition property and increase the emission intensity. Although supramolecular assemblies based on permethylated CDPDI conjugates have been previously reported,[35–38] the formation of assemblies cannot prevent the decrease in the monomer emission intensity of the PDI units due to self-quenching. In addition, the affinity of permethylated CDs with guest molecules significantly decreases compared with native CDs.[39]

Herein we report the selective emission properties of PDI-CD_2 derivatives through the tumbling of the altropyranose unit in an aqueous solution. Previously, we have reported the formation of *pseudo*[1]rotaxane dimer from the *altro*-α-CD (*altro*-α-CD) dimer via tumbling of *altro*-α-CD,[40,41] which consists of one altropyranose unit and five glucopyranose units. Although some research groups have reported the tumbling of permethylated glucopyranose type CD,[42–47] tumbling of the altropyranose unit in *altro*-CDs has yet to be reported. We have successfully observed the selective emission of PDI-CD_2s in aqueous solutions and prepared emission films based on PDI-CD_2s kneaded into polyvinyl alcohol (PVA) films. The emission depends on the cavity size of the *altro*-CDs formed through *altro*-CD tumbling.

EXPERIMENTAL PROCEDURE

Preparation of PDI-6αCD_2

6-NH_2-α-CD (100 mg, 0.103 mmol) and 3,4,9,10-perylene tetracarboxylic dianhydride (20.0 mg, 0.0511 mmol) were dissolved in anhydrous dimethyl formamide (DMF; 10 ml) and stirred at 120 °C for 24 h under Ar atmosphere. Reaction mixture was dried under vacuum and dissolved in 5 ml of water. The solution was poured into acetone (100 ml) and participate was filtered. This precipitate was absorbed on Celite and wash with acetone and chloroform.

Department of Macromolecular Science, Graduate School of Science, Osaka University, Toyonaka, Japan
Correspondence: Professor A Harada, Department of Macromolecular Science, Graduate School of Science, Osaka University, Machikaneyama 1-1, Toyonaka, Osaka 560-0043, Japan.
E-mail: harada@chem.sci.osaka-u.ac.jp
Received 4 September 2011; revised 11 October 2011; accepted 23 October 2011; published online 18 January 2012

After washing, crude product was eluted from Celite with water and purified by DIAION HP-20 reverse phase column (Mitsubishi Chemical Co., Tokyo, Japan, eluent: water to water/methanol=70: 30). Fraction of water/methanol=70:30 was collected and dried to obtain the product as a red solid in the yield of 43.3 mg (36.8%). ^{1}H nuclear magnetic resonance (NMR) and ^{13}C NMR spectra are shown in Supplementary Figures S1 and S2. Contour plot of fluorescence intensity versus excitation and emission wavelengths in DMF or aqueous solution are shown in Supplementary Figures S3 and S4.

Preparation of PDI-6βCD$_2$

PDI-6βCD$_2$ was synthesized in the same manner as PDI-αCD$_2$, using 6-NH$_2$-β-CD (113 mg, 0.103 mmol), 3,4,9,10-perylene tetracarboxylic dianhydride (20.0 mg, 0.0511 mmol) and DMF (10 ml). Crude product was purified by DIAION HP-20 reverse phase column (eluent: water to water/methanol=70:30). The product was obtained as a red solid in the yield of 66.0 mg (49.3%). ^{1}H NMR and ^{13}C NMR spectra are shown in Supplementary Figures S5 and S6. Contour plot of fluorescence intensity versus excitation and emission wavelengths in DMF or aqueous solution are shown in Supplementary Figures S7 and S8.

Preparation of PDI-6γCD$_2$

PDI-γCD$_2$ was synthesized in same manner as PDI-αCD$_2$, using 6-NH$_2$-γ-CD (259 mg, 0.206 mmol), 3,4,9,10-perylene tetracarboxylic dianhydride (40.0 mg, 0.102 mmol) and DMF (20 ml). Crude product was purified by DIAION HP-20 reverse phase column (eluent: water to water/methanol=70:30). The product was obtained as a red solid in the yield of 53.4 mg (18.1%). ^{1}H NMR and ^{13}C NMR spectra are shown in Supplementary Figures S9 and S10. Contour plot of fluorescence intensity versus excitation and emission wavelengths in DMF or aqueous solution are shown in Supplementary Figures S11 and S12.

Preparation of PDIC$_7$-3αCD$_2$

N,*N*'-bis(6-carboxylhexyl)perylene-3,4,9,10-tetracarboxyl diimide (32.3 mg, 0.050 mmol), 3-NH$_2$-α-CD (97.2 mg, 0.100 mmol), PyBOP (57.2 mg, 0.110 mmol) and a drop of triethylamine were dissolved in DMF and stirred at room temperature for 48 h. DMF was evaporated and residue was dissolved in a small amount of water. Aqueous solution was poured in acetone (50 ml) and precipitate was collected (this manipulation was repeated three times). Crude product was purified by DIAION HP-20 reverse phase column (eluent: water to water/methanol=50:50). Fraction of water/methanol=50:50 was collected and dried to obtain the product as a red solid in the yield of 25.6 mg (20.0%). ^{1}H NMR and ^{13}C NMR spectra are shown in Supplementary Figures S14 and S15. Contour plot of fluorescence intensity versus excitation and emission wavelengths in DMF or aqueous solution are shown in Supplementary Figures S17 and S18.

Preparation of PDIC$_7$-3βCD$_2$

PDIC$_7$-3βCD$_2$ was synthesized in same manner as PDIC$_7$-αCD$_2$, using 3-NH$_2$-β-CD (113 mg, 0.100 mmol). Crude product was purified by DIAION HP-20 reverse phase column (eluent: water to water/methanol=50:50). Fraction of water/methanol=60:40 was collected and dried to obtain the product as a red solid in the yield of 43.6 mg (30.3%). ^{1}H NMR and ^{13}C NMR spectra are shown in Supplementary Figures S19 and S20. Contour plot of fluorescence intensity versus excitation and emission wavelengths in DMF or aqueous solution are shown in Supplementary Figures S22 and S23.

Preparation of PDIC$_7$-3γCD$_2$

PDIC$_7$-3γCD$_2$ was synthesized in same manner as PDIC$_7$-3αCD$_2$, using 3-NH$_2$-γ-CD (130 mg, 0.100 mmol). Crude product was purified by DIAION HP-20 reverse phase column (eluent: water to water/methanol=50: 50). Fraction of water/methanol=70:30 was collected and dried to obtain the product as a red solid in the yield of 33.0 mg (20.6%). ^{1}H NMR and ^{13}C NMR spectra are shown in Supplementary Figures S23 and S24. Contour plot of fluorescence intensity versus excitation and emission wavelengths in DMF or aqueous solution are shown in Supplementary Figures S27 and S28.

Preparation of PVA films with PDI-CD$_2$s

The 300 μl of aqueous solution of PDI-CD$_2$s (1 mM) was dropped on the Teflon petri. The 8 g of poly(vinyl alcohol) (M_n=2000) aqueous solution (10 wt%) was added to the PDI-CD$_2$s aq. The PVA films with PDI-CD$_2$s were obtained by evaporating the water at 75 °C in a thermostatic chamber.

RESULTS

Preparation and chemical structures of PDI-6CD$_2$s and PDIC$_7$-3CD$_2$s

Figure 1 shows the six different PDI-CDs. PDI-6CD$_2$s (PDI-6αCD$_2$, PDI-6βCD$_2$ and PDI-6γCD$_2$) are directly crosslinked between CDs with PDI. PDI-6CD$_2$s were prepared by the reaction of 6-amino-CDs with perylene dicarboxylic acid dihydride. PDIC$_7$-3CD$_2$s (PDIC$_7$-

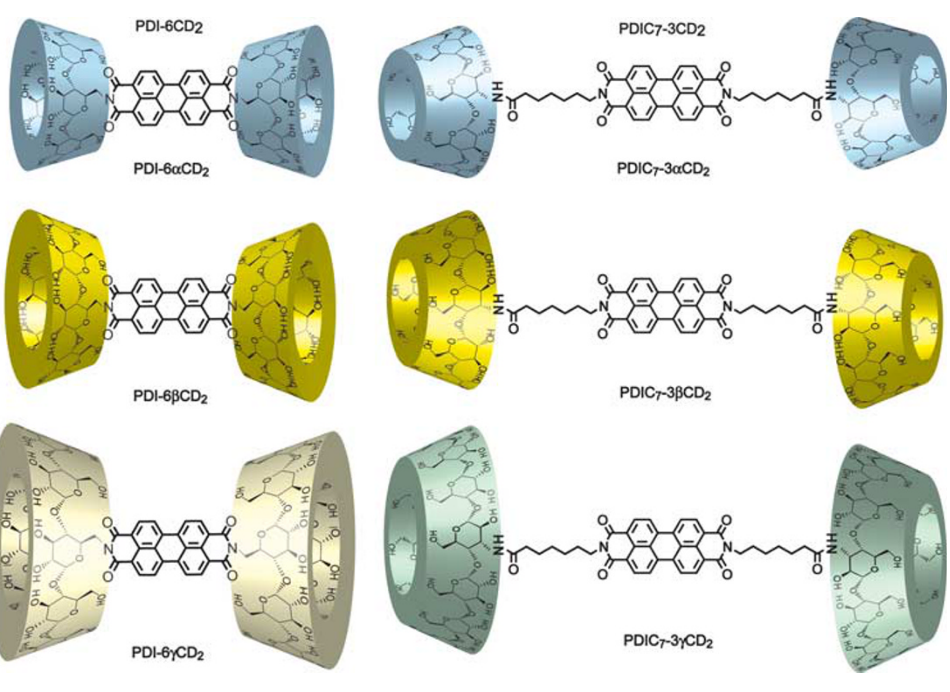

Figure 1 Chemical structures of PDI-6CD$_2$s and PDIC$_7$-3CD$_2$s.

3αCD$_2$, PDIC$_7$-3βCD$_2$ and PDIC$_7$-3γCD$_2$) were prepared by the reaction of 3-amino-CDs with *N*,*N*'-bis(6-carboxylhexyl)perylene-3,4,9,10-tetracarboxyl diimide (BisC$_7$-PDI, see in Supplementary information in Supplementary Figure S13.) using 4-(4,6-dimethoxy-1,3,5-triazin-2-yl)-4-methylmorpholinium chloride (DMT-MM). The photophysical properties of PDI-6CD$_2$ and PDIC$_7$-3CD$_2$ were characterized by absorption and fluorescence spectroscopies. The supramolecular structures of PDI–CD derivatives were characterized by ^{1}H NMR spectroscopic methods.

Absorption and fluorescence properties of PDI-6CD$_2$s

Figures 2 and 3 show the absorption and fluorescence spectra of PDI-6CD$_2$s in DMF and aqueous solutions, respectively. The absorption and fluorescence spectra of PDI-6CD$_2$s in DMF are similar regardless of the type of CD. Table 1 summarizes the quantum yields (Φ_{em}) of PDI-6CD$_2$s and PDIC$_7$-3CD$_2$s in DMF and water. The Φ_{em} values of PDI-6αCD$_2$ and PDI-6βCD$_2$ are slightly higher than that of PDI-6γCD$_2$ in DMF. On the other hand, the fluorescence intensities of PDI-6CD$_2$s in aqueous solutions significantly decrease due to self-quenching. The difference in the fluorescence intensities and Φ_{em} of PDI-6CD$_2$s are due to self-aggregation. Φ_{em} of PDI-6γCD$_2$ is higher than those of PDI-6αCD$_2$ and PDI-6βCD$_2$, and this higher value is related to the inhibition of self-aggregation through π–π stacking interactions due to the bulkiness of γ-CD in aqueous solutions.

Absorption and fluorescence properties of PDIC$_7$-3CD$_2$

PDIC$_7$-3CD$_2$s exhibit unpredictable specific emission behaviors in aqueous solutions. First, we investigated the dependence of the

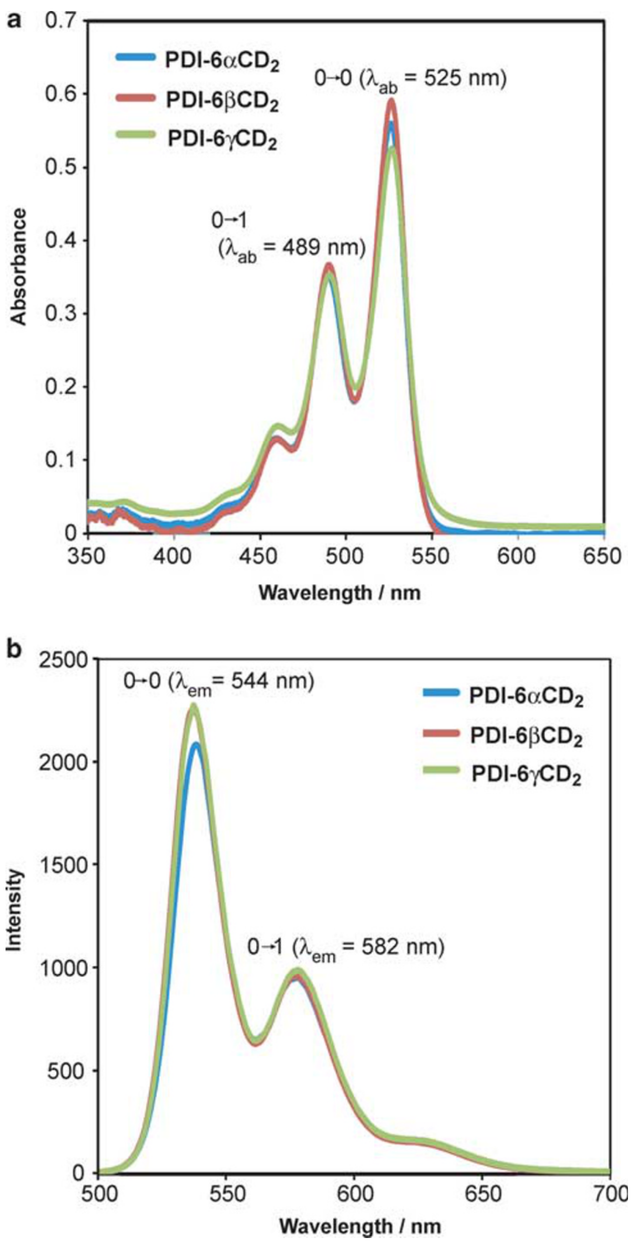

Figure 2 Absorption (a) and fluorescence (b) spectra of PDI-6CD$_2$s in DMF. Concentrations are adjusted to 15 μM. Samples in fluorescence measurements are excited at λ_{ex}=489 nm.

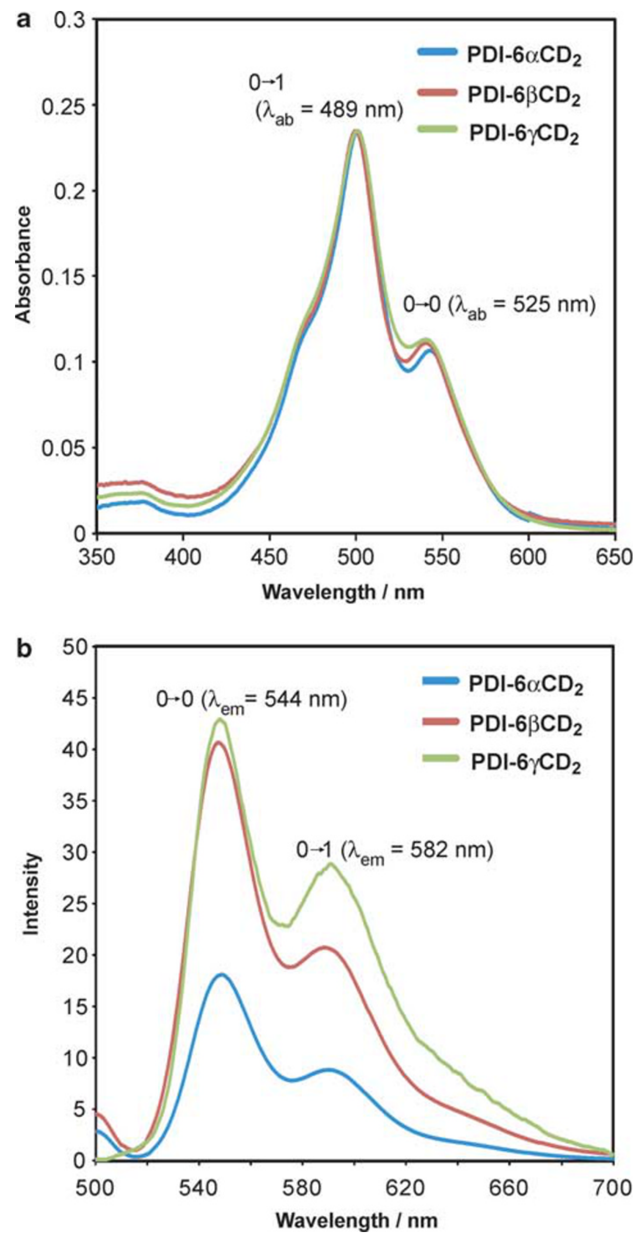

Figure 3 Absorption (a) and fluorescence (b) spectra of PDI-6CD$_2$s in water. Concentrations are adjusted to 15 μM. Samples in fluorescence measurements are excited at λ_{ex}=495 nm.

Table 1 Photophysical properties of PDI-6CD$_2$s and PDIC$_7$-3CD$_2$s[a]

PDI-CD$_2$	*Solvent*	*λ_{abs}/nm 0→0/ 0→1*	*S ($A^{0\to1}$/ $A^{0\to0}$)*	*λ_{em}/ nm[b]*	*Φ_{em}/ %[c]*	*Lifetime[d] τ/ns*	*χ^2*
PDI-6αCD$_2$	DMF	526/490	0.63	538	70	—	—
	H_2O	543/501	2.21	549	1.3	—	—
PDI-6βCD$_2$	DMF	526/490	0.62	537	71	—	—
	H_2O	540/500	2.12	547	2.4	—	—
PDI-6γCD$_2$	DMF	526/490	0.67	537	73	—	—
	H_2O	540/501	2.08	548	4.2	—	—
PDIC$_7$-3αCD$_2$	DMF	525/489	0.65	539	71	3.6±0.03[e]	1.32
	H_2O	544/499	2.05	547	0.90	—	—
PDIC$_7$-3βCD$_2$	DMF	525/489	0.64	539	72	3.6±0.02[e]	1.22
	H_2O	530/494	0.74	544	43	3.6±0.2[e]	1.29
PDIC$_7$-3γCD$_2$	DMF	525/489	0.66	539	64	3.7±0.03[e]	1.48
	H_2O	529/498	1.25	544	11	~2.6, 6.1[f]	1.19

Abbreviations: CD, cyclodextrin; DMF, dimethyl formamide; PDI, perylene diimide.
[a]Measured in a degassed aqueous solution at 25 °C.
[b]Emission maximum.
[c]Absolute fluorescence quantum yield of emission is measured by excitation at 500 nm.
[d]Fluorescence spectra are analyzed by a streak-camera system attached to a 15-cm spectrometer.
[e]Fluorescence decays are fitted by single-component model.
[f]Fluorescence decay of PDIC$_7$-3γCD$_2$ in H_2O is fitted by two-component model (see Supporting information, Supplementary Figure S28).

photophysical properties of PDIC$_7$-3CD$_2$s on the solvent. Figure 4, which shows the absorption and fluorescence spectra of PDIC$_7$-3CD$_2$s in DMF, demonstrates that the absorption and fluorescence spectra of PDIC$_7$-3CD$_2$s are similar for all the CDs. However, in aqueous solutions, the absorption band of PDIC$_7$-3CD$_2$s depends on the CD cavity (Figure 5). The absorption band of PDIC$_7$-3βCD$_2$ exhibits distinctive vibrational-electronic coupling and vibronic transitions on top of the allowed π–π* electronic transition can be resolved, whereas PDIC$_7$-3αCD$_2$ and PDIC$_7$-3γCD$_2$ display broad absorption bands. Φ_{em} of PDIC$_7$-3βCD$_2$ is significantly higher than those of PDIC$_7$-3αCD$_2$ and PDIC$_7$-3γCD$_2$ (Table 1). Φ_{em} of PDIC$_7$-3βCD$_2$ in an aqueous solution is close to that of PDIC$_7$-3βCD$_2$ in DMF.

Due to π-stacking interactions, large aromatic ring derivatives can easily form supramolecular assemblies. Hence, the strong intermolecular vibrational-electronic coupling in PDI derivatives has been well studied.[6,16–21] The formation of PDI assemblies leads to broad vibrational-electronic coupling due to fused aromatic rings whose molecular orbital overlap with adjacent neighbors. In contrast, free PDI derivatives provide clear vibrational-electronic coupling. The Huang–Rhys factor, $S=A^{0\to1}/A^{0\to0}$ ($A^{0\to0}$, absorption intensity of 0→0 band; $A^{0\to1}$, absorption intensity of 0→1 band), is an indicator of the formation of supramolecular assemblies.[6,16–21] The intensities of 0→0 band ($A^{0\to0}$) and 0→1 band ($A^{0\to1}$) in DMF do not have a measurable difference between PDIC$_7$-3CD$_2$s (Figure 4), whereas the intensities in aqueous solutions depend on the CD cavity (Figure 5). The *S* ratio of PDIC$_7$-3βCD$_2$ in an aqueous solution is similar to that in DMF (S=0.74 (aq), S=0.64 (DMF)). The *S* ratios of PDIC$_7$-3γCD$_2$ in aqueous solutions is 1.25, which is the value intermediate between PDIC$_7$-3αCD$_2$ and PDIC$_7$-3βCD$_2$ in aqueous solutions. The *S* ratios of PDIC$_7$-3αCD$_2$ in aqueous solutions is 2.05, which is close to those of PDI-6CD$_2$s in aqueous solutions.

Although the association behavior of PDIC$_7$-3αCD$_2$ is similar to the values for known PDI derivatives,[5–21] PDIC$_7$-3βCD$_2$ shows a definite emission, suggesting that PDIC$_7$-3βCD$_2$ is relatively dispersed even in aqueous solutions. PDIC$_7$-3αCD$_2$ and PDIC$_7$-3γCD$_2$ do not show

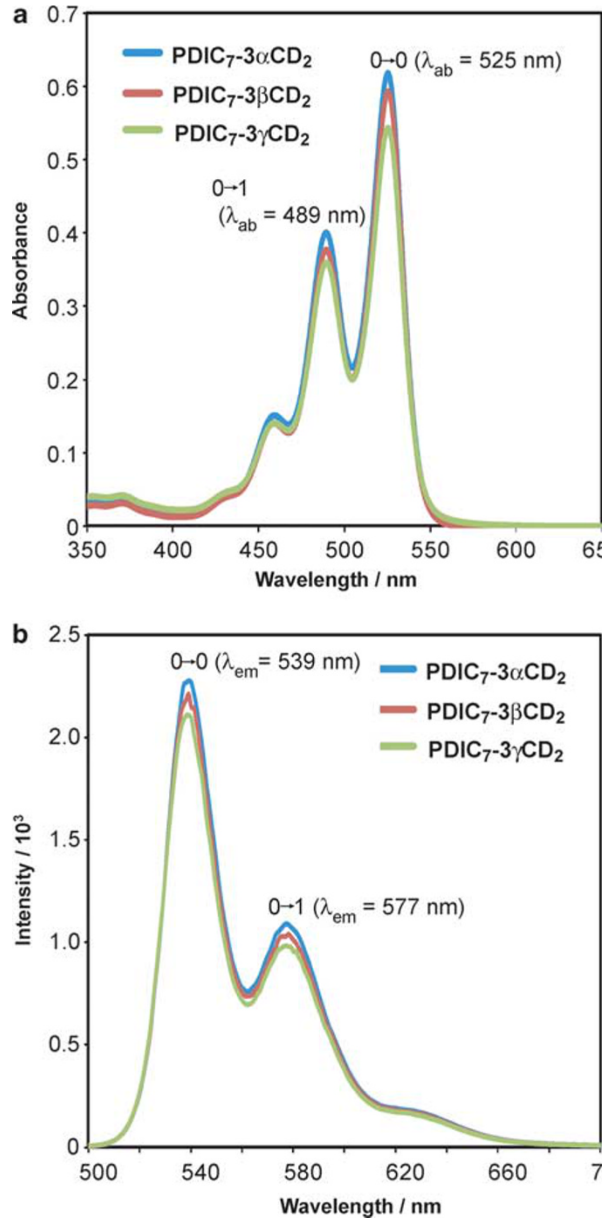

Figure 4 Absorption (**a**) and fluorescence (**b**) spectra of PDIC$_7$-3CD$_2$ in DMF. Concentrations are adjusted to 15 μM. Samples in fluorescence measurements are excited at λ_{ex}=489 nm.

distinctive quantum yields (Φ_{em}=0.90 and 11%). However, Φ_{em} of PDIC$_7$-3βCD$_2$ is 43%, which is close to that in DMF. These results indicate that PDIC$_7$-3CD$_2$s are effectively dispersed and form monomers in DMF, but PDIC$_7$-3αCD$_2$ and PDIC$_7$-3γCD$_2$ form supramolecular assemblies in aqueous solutions. However, PDIC$_7$-3βCD$_2$ is effectively dispersed even in an aqueous solution.

Supramolecular structure of PDIC$_7$-3CD$_2$s

We hypothesized that the emission differences are due to the formation of supramolecular complexes. The two-dimensional rotating-frame overhauser spectroscopy spectrum of PDIC$_7$-3αCD$_2$ indicates the C7 alkyl unit and the inner protons of *altro*-α-CD end groups are correlated, but the PDI unit and inner protons in aqueous solutions

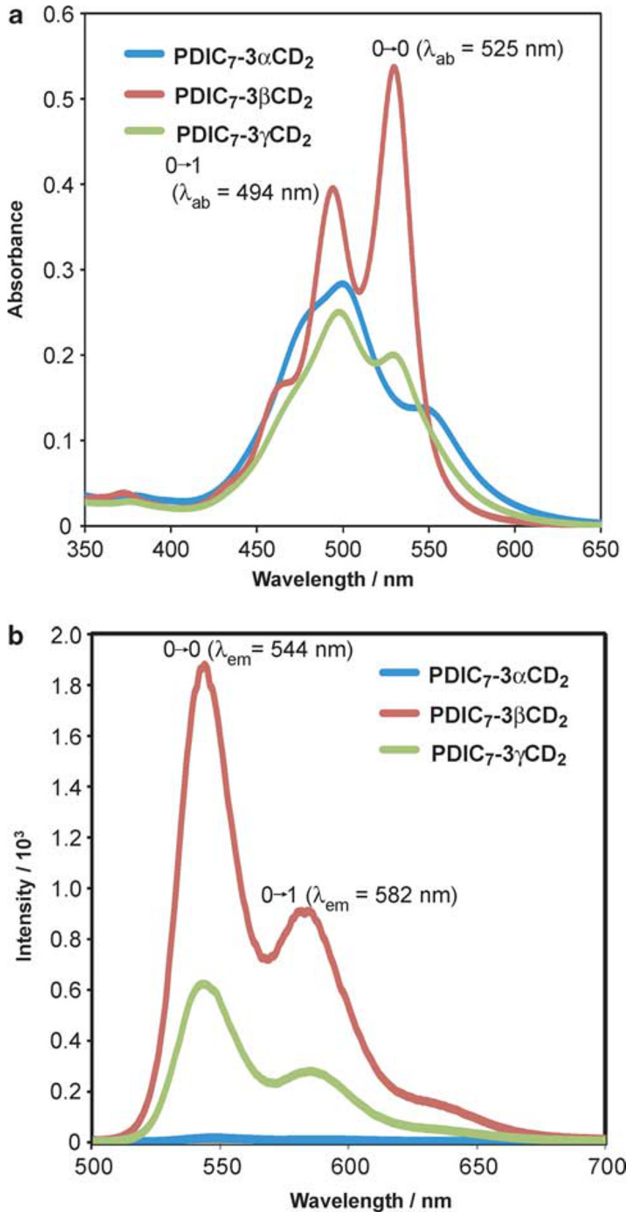

Figure 5 Absorption (**a**) and fluorescence (**b**) spectra of PDIC$_7$-3CD$_2$s in water. Concentrations are adjusted to 15 μM. Samples in fluorescence measurements are excited at λ_{ex}=494 nm.

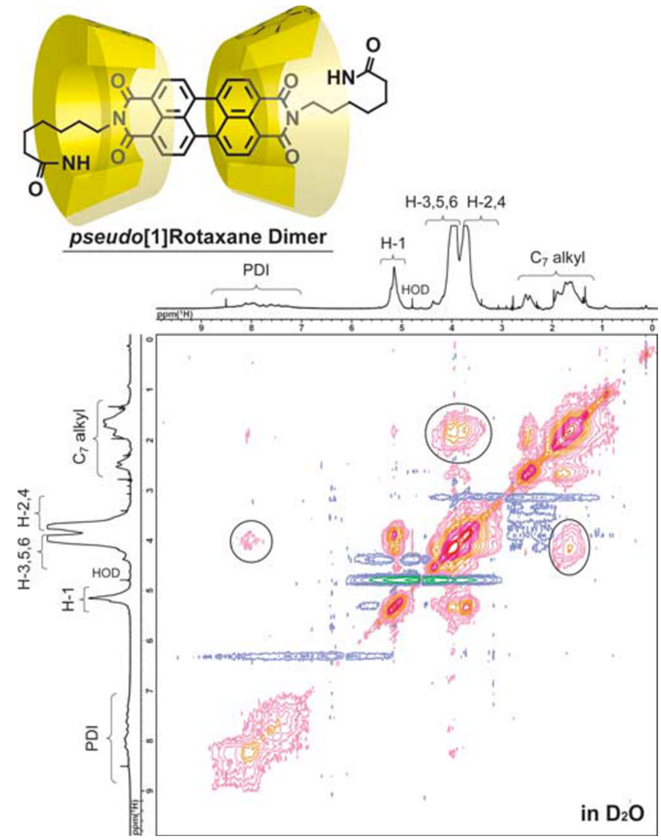

Figure 6 Two-dimensional nuclear overhauser effect spectroscopy NMR spectrum of PDIC$_7$-3βCD$_2$ in D$_2$O (1 mM) at 30 °C (mixing time=150 ms) and proposed structure of the *pseudo*[1]rotaxane dimer from PDIC$_7$-3βCD$_2$ in water.

are not (see Supporting information in Supplementary Figure S16). The two-dimensional rotating-frame overhauser spectroscopy spectrum of PDIC$_7$-3βCD$_2$ demonstrates that the inner protons of *altro*-β-CD are correlated to the protons of PDI and C7 alkyl units (Figure 6). The two-dimensional rotating-frame overhauser spectroscopy spectrum of PDIC$_7$-3γCD$_2$ shows the *altro*-γ-CD inner protons are correlated to the protons of PDI and C7 alkyl units (Supplementary Figure S25). These results show that the *altro*-CD unit includes the C$_7$PDI axis molecule in aqueous solutions.

How is the *altro*-CD unit included the C$_7$PDI axis molecule in the cavity? PDIC$_7$-3CD$_2$s are regarded to have a dumbbell shape. Other CD molecules cannot physically slip through the end of the *altro*-CDs of PDIC$_7$-3CD$_2$s to form *pseudo*[2]rotaxane. Previously, we have reported that an alkyl *altro*-α-CD dimer is converted into a *pseudo*[1]rotaxane dimer through tumbling of the altropyranose unit of *altro*-α-CD in D$_2$O.[40,41] On the basis of these results, PDIC$_7$-3βCD$_2$ forms a *pseudo*[1]rotaxane dimer through tumbling of the altropyranose unit of *altro*-β-CD in aqueous solutions (Scheme 1).

PDIC$_7$-3αCD$_2$ forms a *pseudo*[1]rotaxane dimer, which includes the C7 alkyl unit in the *altro*-α-CD cavity (Scheme 2). The cavity size of *altro*-α-CD is too small to include the PDI unit. *Altro*-β-CD and *altro*-γ-CD possess a sufficient cavity size to include the PDI unit. PDIC$_7$-3βCD$_2$ and PDIC$_7$-3γCD$_2$ form *pseudo*[1]rotaxane dimmers, where the PDI unit is covered by the *altro*-CDs end groups. Coverage of the PDI unit inhibits the π–π stacking interaction between PDI units, leading to self-quenching. In contrast, PDIC$_7$-3αCD$_2$ cannot inhibit self-quenching due to the defective coverage of the PDI unit. Actually, we have investigated the inhibition of *altro*-β-CD tumbling using a competitive guest, adamantane carboxylic acid sodium salt, which is strongly included in the cavity of β-CD.[39,48–52] Mixing 100 equivalents of adamantane carboxylic acid sodium salt guest molecules with a PDIC$_7$-3βCD$_2$ aqueous solution decreases the emission intensities of PDIC$_7$-3βCD$_2$ (Supplementary Figure S29). The addition of an excess of adamantane carboxylic acid sodium salt into a PDIC$_7$-3βCD$_2$ aqueous solution causes a marked decrease in the emission intensity, which is 61% of the initial intensity. Hence, adamantane carboxylic acid sodium salt included in the *altro*-β-CD unit of PDIC$_7$-3βCD$_2$ inhibits tumbling of the altropyranose unit.

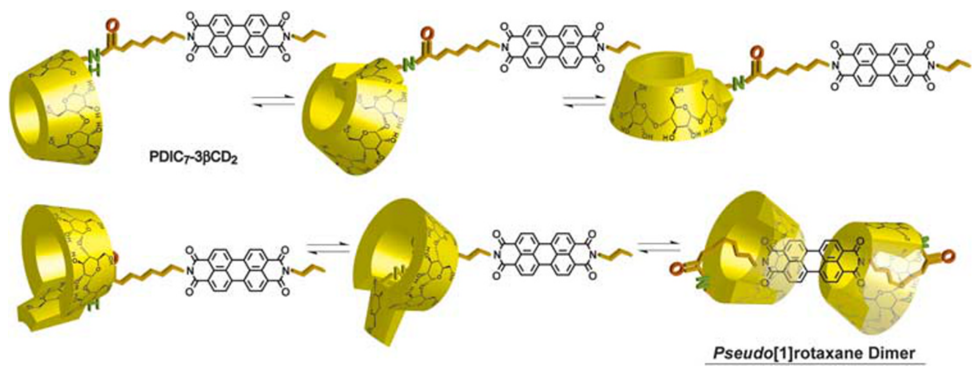

Scheme 1 Formation of the *pseudo*[1]rotaxane dimer from PDIC$_7$-3βCD$_2$ via tumbling of the altropyranose unit.

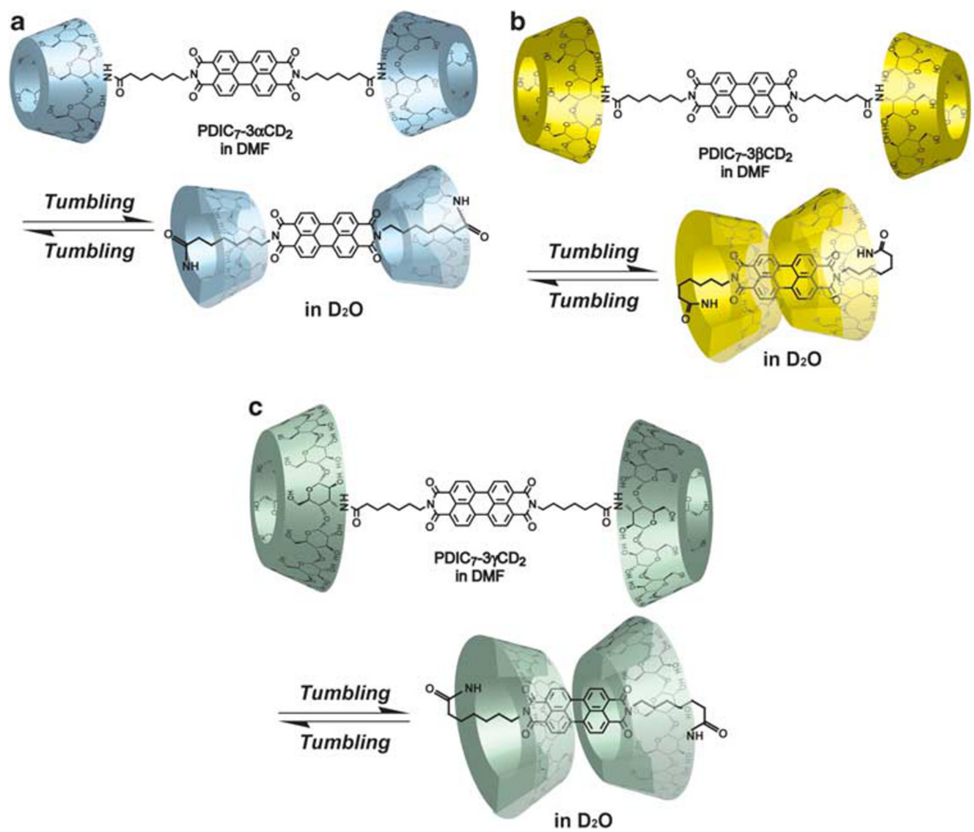

Scheme 2 Schematic illustration of the solvent polarity dependent formation of the *pseudo*[1]rotaxane dimer from PDIC$_7$-3αCD$_2$ (**a**), PDIC$_7$-3βCD$_2$ (**b**), and PDIC$_7$-3γCD$_2$ (**c**).

Association constants of CDs with BisC$_7$-PDI

To investigate the differences in the correlation peaks of the two-dimensional nuclear overhauser effect spectroscopy NMR spectra and the emission intensities for the various CDs, the stoichiometric proportion and the association constants were determined by UV titration measurements (see Supporting Information, Supplementary Figures S33–S35). Job's plots suggest that each CD forms a 2:1 complex for BisC$_7$-PDI in aqueous solutions. (see Supporting information, Supplementary Figures S30–S32) The K_1 values of α-CD and γ-CD with BisC$_7$-PDI are $6.2\times10^4\,\mathrm{M}^{-1}$ and $1.5\times10^5\,\mathrm{M}^{-1}$, respectively, whereas that of β-CD with BisC$_7$-PDI is larger ($4.0\times10^5\,\mathrm{M}^{-1}$; Table 2) These results indicate that the emission intensity of PDIC$_7$-3βCD$_2$ is selectively higher than those of PDIC$_7$-3αCD$_2$ and PDIC$_7$-3γCD$_2$ due to the suppression of self-aggregation.

Emission properties of PDIC$_7$-3CD$_2$ films

Figure 7 shows photographs of PDIC$_7$-3CD$_2$s in aqueous solutions. The emission intensities do not differ for PDIC$_7$-3CD$_2$s in DMF solutions, whereas in aqueous solutions, only PDIC$_7$-3βCD$_2$ shows a distinct green–yellow emission.

Using the emission properties in aqueous solutions, we prepared a PVA film with PDIC$_7$-3CD$_2$s. An aqueous solution of PDIC$_7$-3CD$_2$s (0.3 μmol) was mixed with an aqueous solution of PVA (0.80 g), and subsequently dried at 75 °C (see Supporting information, Supplementary Figure S36). Although the resulting PVA films with PDIC$_7$-3CD$_2$s are slightly red, they are the same under visible light (Figure 8). Only the film with PDIC$_7$-3βCD$_2$ shows a bright yellow emission under UV light. PVA films with PDIC$_7$-3αCD$_2$ and PDIC$_7$-3γCD$_2$ do not display distinct emissions; actually, the PDIC$_7$-3αCD$_2$ and PDIC$_7$-3γCD$_2$ films do not show distinct quantum yields (Φ_{em}=14 and 24%), but Φ_{em} of a film of PDIC$_7$-3βCD$_2$ is 54%. The PVA film with PDIC$_7$-3βCD$_2$ can be prepared from the dimethyl sulfoxide solutions, but this method is unsuited for a homogeneous, large-area film with a flat surface (Figure 8d). Dropping a PDIC$_7$-3βCD$_2$ aqueous solution onto a quartz plate and subsequent drying in air produce a PDIC$_7$-3βCD$_2$ solid that exhibits a weak red light instead of a bright yellow emission under UV light (λ_{ex}=365 nm; see Supporting information, Supplementary Figure S37).

PDIC$_7$-3βCD$_2$ is self-quenching in the solid state due to self-aggregation through a π–π stacking interaction. First, we speculated that the emission intensity differences between PDIC$_7$-3CD$_2$s would not be observed in PVA films, because the structure of the *pseudo*[1]rotaxane dimer from PDIC$_7$-3βCD$_2$ would decompose in the PVA matrix. However, the supramolecular structure of PDIC$_7$-3βCD$_2$ remains in the PVA films. Only the PDIC$_7$-3βCD$_2$ film shows a bright green−yellow emission under UV light.

Table 2 Association constants of CDs with BisC$_7$-PDI in aqueous solutions

CD	*K$_1$/M*	*K$_2$/M*
α-CD	6.2×10^4	2.1×10^3
β-CD	4.0×10^5	1.5×10^3
γ-CD	1.5×10^5	3.4×10^3

Abbreviations: CD, cyclodextrin; PDI, perylene diimide.

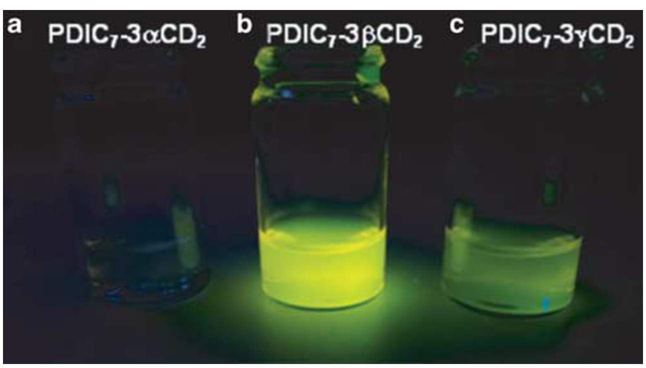

Figure 7 Emission properties of PDIC$_7$-3αCD$_2$ (**a**), PDIC$_7$-3βCD$_2$ (**b**) and PDIC$_7$-3γCD$_2$ (**c**) in aqueous solutions under UV light (λ_{ex}=365 nm).

DISCUSSION

We prepared CD-PDI derivatives where the emission properties depend on the type of CD. Although PDI derivatives usually have low solubilities in aqueous solutions, the introduction of the CD units improves the solubility. PDI-6CD$_2$s, in which the CD unit is directly introduced into the PDI unit without spaces, dissolves in water, but does not show an emission difference with the type of CD unit. In contrast to PDI-6CD$_2$s, PDIC$_7$-3βCD$_2$ displays a bright yellow emission and PDIC$_7$-3γCD$_2$ has a weak emission. The emission properties of PDIC$_7$-3CD$_2$s are due to the tumbling of the altropyranose unit, which prevents self-aggregation and self-quenching in aqueous solutions.

To utilize the selective emission properties, PVA films woven with PDIC$_7$-3CD$_2$s were prepared. Even in PVA films, PDIC$_7$-3CD$_2$s show selective emission behaviors, which depend on the CD. We initially speculated that the *pseudo*[1]rotaxane dimer would decompose to the original dimer in the film, and the emission differences according to the type of CD would not be observed. However, the opposite results are observed, indicating PDIC$_7$-3βCD$_2$ forms *pseudo*[1]rotaxane dimers even in PVA films. The PVA films with PDIC$_7$-3βCD$_2$ should function as emission and quenching sensor films for chemical compounds based on the molecular recognition property of CDs.

ACKNOWLEDGEMENTS

We thank Mr S Adachi (Osaka University) for his support of the 2D-NMR experiments. This work was supported by the 'Core Research for Evolutional Science and Technology' program of the Japan Science and Technology Agency, Japan.

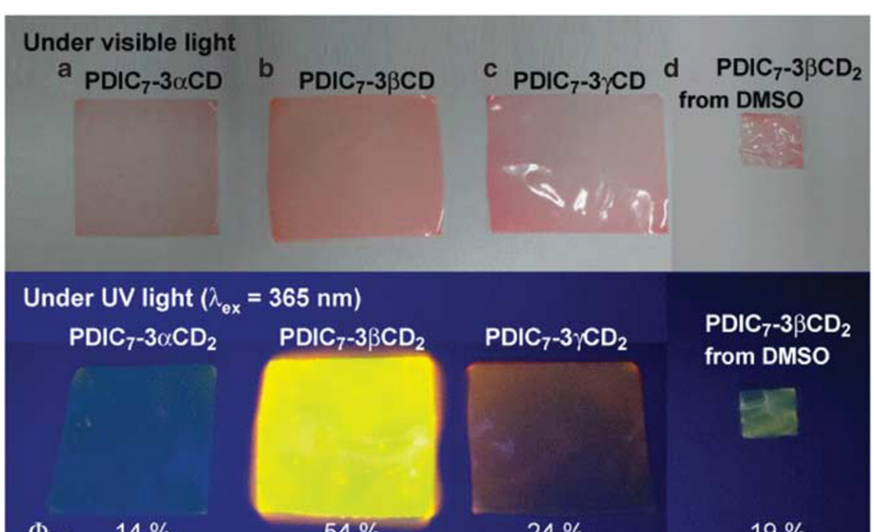

Figure 8 Emission properties of PVA films dissolved PDIC$_7$-3αCD$_2$ (**a**), PDIC$_7$-3βCD$_2$ (**b**), and PDIC$_7$-3γCD$_2$ (**c**), under visible light and UV light (λ_{ex}=365 nm). PVA film (**d**) is prepared via a dimethyl sulfoxide solution of PDIC$_7$-3βCD$_2$.

1 Smulders, M. M. J., Schenning, P. H. J. & Meijer, E. W. Insight into the mechanisms of cooperative self-assembly: the Sergeants-and-Soldiers Principle of Chiral and Achiral C3-Symmetrical Discotic Triamides. *J. Am. Chem. Soc.* **130,** 606–611 (2008).
2 Meyer, E. A., Castellano, R. K. & Diederich, F. Interactions with aromatic rings in chemical and biological recognition. *Angew. Chem. Int. Ed.* **42,** 1210–1250 (2003).
3 Busch, D. H. First considerations: principles, classification, and history of templates. *Top. Curr. Chem.* **249,** 1–65 (2005).
4 Gabriel, G. J., Sorey, S. & Iverson, B. L. Altering the folding patterns of naphthyl trimers. *J. Am. Chem. Soc.* **127,** 2637–2640 (2005).
5 Su, W., Zhang, Y., Zhao, C., Li, X. & Jiang, J. Self-assembled organic nanostructures: effect of substituents on the morphology. *Chemphyschem* **8,** 1857–1862 (2007).
6 Wang, W., Han, J. J., Wang, L. Q., Li, L. S., Shaw, W. J. & Li, A. D. Q. Dynamic pi-pi stacked molecular assemblies emit from green to red colors. *Nano Lett.* **3,** 455–458 (2003).
7 Chen, Z. J., Stepanenko, V., Dehm, V., Prins, P., Siebbeles, L. D., Seibt, J., Marquetand, P., Engel, V. & Würthner, F. Photoluminescence and conductivity of self-assembled π-π stacks of perylene bisimide dyes. *Chem. Eur. J.* **13,** 436–449 (2007).
8 Langhals, H. & Jona, W. Intense dyes through chromophore-chromophore interactions: bi- and trichromophoric perylene-3,4:9,10-bis(dicarboximide)s. *Angew. Chem. Int. Ed.* **37,** 952–955 (1998).
9 Würthner, F., Thalacker, C., Diele, S. & Tschierske, C. Fluorescent J-type aggregates and thermotropic columnar mesophases of perylene bisimide dyes. *Chem. Eur. J.* **7,** 2245–2253 (2001).
10 Yagai, S., Seki, T., Karatsu, T., Kitamura, A. & Würthner, F. Transformation from H- to J-aggregated perylene bisimide dyes by complexation with cyanurates. *Angew. Chem. Int. Ed.* **47,** 3367–3371 (2008).
11 Giaimo, J. M., Lockard, J. V., Sinks, L. E., Scott, A. M., Wilson, T. M. & Wasielewski, M. R. Excited Singlet States of Covalently Bound, Cofacial Dimers and Trimers of Perylene-3,4:9,10-bis(dicarboximide)s. *J. Phys. Chem. A.* **112,** 2322–2330 (2008).
12 Rybtchinski, B., Sinks, L. E. & Wasielewski, M. R. Photoinduced Electron Transfer in Self-Assembled Dimers of 3-Fold Symmetric Donor-Acceptor Molecules Based on Perylene-3,4:9,10-bis(dicarboximide). *A. J. Phys. Chem.* **108,** 7497–7505 (2004).
13 Chen, Z., Baumeister, U., Tschierske, C. & Wurthner, F. Effect of core twisting on self-assembly and optical properties of perylene bisimide dyes in solution and columnar liquid crystalline phases. *Chem. Eur. J.* **13,** 450–465 (2007).
14 Ahrens, M. J., Sinks, L. E., Rybtchinski, B., Liu, W., Jones, B. A., Giaimo, J. M., Gusev, A. V., Goshe, A. J., Tiede, D. M. & Wasielewski, M. R. Self-assembly of supramolecular light-harvesting arrays from covalent multi-chromophore perylene-3,4: 9,10-bis(dicarboximide) building blocks. *J. Am. Chem. Soc.* **126,** 8284–8294 (2004).
15 Li, Y., Li, Y., Li, J., Li, C., Liu, X., Yuan, M., Liu, H. & Wang, S. Synthesis, characterization, and self-assembly of nitrogen-containing heterocoronenetetracarboxylic acid diimide analogues: Photocyclization of N-heterocycle-substituted perylene bisimides. *Chem. Eur. J.* **12,** 8378–8385 (2006).
16 Wang, W., Li, L. S., Helms, G., Zhou, H. H. & Li, A. D. Q. To fold or to assemble? *J. Am. Chem. Soc.* **125,** 1120–1121 (2003).
17 Li, A. D. Q., Wang, W. & Wang, L. Q. Folding versus self-assembling. *Chem. Eur. J.* **9,** 4594–4601 (2003).
18 Wang, W., Wang, L. Q., Palmer, B. J., Exarhos, G. J. & Li, A. D. Q. Cyclization and Catenation Directed by Molecular Self Assembly. *J. Am. Chem. Soc.* **128,** 11150–11159 (2006).
19 Han, J. J., Wang, W. & Li, A. D. Q. Folding and Unfolding of Chromophoric Foldamers Show Unusual Colorful Single Molecule Spectral Dynamics. *J. Am. Chem. Soc.* **128,** 672–673 (2006).
20 Han, J. J., Shaller, A. D., Wang, W. & Li, A. D. Q. Architecturally diverse nanostructured foldamers reveal insightful photoinduced single-molecule dynamics. *J. Am. Chem. Soc.* **130,** 6974–6982 (2008).
21 Wang, W., Bain, A. D., Wang, L. Q., Exarhos, G. J. & Li, A. D. Q. Molecular Self-Assembly Inhibition Leads to Basket-Shaped Cyclophane Formation with Chiral Dynamics. *J. Phys. Chem. A.* **112,** 3094–3103 (2008).
22 Hippius, C., van Stokkum, I. H. M., Zangrando, E., Williams, R. M., Wykes, M., Beljonne, D. & Würthner, F. Ground- and excited-state pinched cone equilibria in calix[4]arenes bearing two perylene bisimide dyes. *J. Phys. Chem. C* **112,** 14626–14638 (2008).
23 Hippius, C., Schlosser, F., Vysotsky, M. O., Bhmer, V. & Würthner, F. Energy Transfer in Calixarene-Based Cofacial-Positioned Perylene Bisimide Arrays. *J. Am. Chem. Soc.* **128,** 3870–3871 (2006).
24 Siekierzycka, J. R., Hippius, C., Würthner, F., Williams, R. M. & Brouwer, A. M. Polymer Glass Transitions Switch Electron Transfer in Individual Molecules. *J. Am. Chem. Soc.* **132,** 1240–1242 (2010).
25 Anh, N. V., Schlosser, F., Groeneveld, M. M., van Stokkum, I. H. M., Würthner, F. & Williams, R. M. Photoinduced interactions in a pyrene-calix[4]arene-perylene bisimide dye system: Probing ground-state conformations with excited-state dynamics of charge separation and recombination. *J. Phys. Chem. C* **113,** 18358–18368 (2009).
26 Hippius, C., van Stokkum, I. H. M., Gsnger, M., Groeneveld, M. M., Williams, R. M. & Würthner, F. Sequential FRET processes in calix[4]arene-linked orange-red-green perylene bisimide dye zigzag arrays. *J. Phys. Chem. C* **112,** 2476–2486 (2008).
27 Vysotsky, M. O., Bhmer, V., Würthner, F., You, C.- C. & Rissanen, K. Calix[4]arene-functionalized naphthalene and perylene imide dyes. *Org. Lett.* **4,** 2901–2904 (2002).
28 Bender, M. L. & Komiyama, M. *Cyclodextrin Chemistry; Reactivity and Structure Concepts in Organic Chemistry* Vol. 6 (Springer: Berlin, Germany, 1978).
29 Szejtli, J *Cyclodextrins and Their Inclusion Complexes* (Akadémiai Kiadó: Budapest, Hungary, 1982).
30 Szejtli, J & Osa, T. (eds) *Comprehensive Supramolecular Chemistry, Cyclodextrins* Vol. 3 (Pergamon: Oxford, UK, 1996).
31 Easton, C. J. & Lincoln, S. F. *Modified Cyclodextrins: Scaffolds and Templates for Supramolecular Chemistry* (Imperial College Press: London, UK, 1999).
32 Harada, A., Hashidzume, A. & Takashima, Y. Cyclodextrin-based supramolecular polymers. *Adv. Polym. Sci.* **201,** 1–43 (2006).
33 Harada, A., Takashima, Y. & Yamaguchi, H. Cyclodextrin-based supramolecular polymers.. *Chem. Soc. Rev.* **38,** 875–882 (2009).
34 Harada, A., Hashidzume, A., Yamaguchi, H. & Takashima, Y. CD-based polymeric rotaxanes. *Chem. Rev.* **109,** 5974–6023 (2009).
35 Liu, Y., Wang, K.- R., Guo, D.- S. & Jiang, B.- P. Supramolecular assembly of perylene bisimide with β-cyclodextrin grafts as a solid-state fluorescence sensor for vapor detection. *Adv. Funct. Mater.* **19,** 2230–2235 (2009).
36 Jiang, B.- P., Guo, D.- S. & Liu, Y. Self-Assembly of Amphiphilic Perylene-Cyclodextrin Conjugate and Vapor Sensing for Organic Amines. *J. Org. Chem.* **75,** 7258–7264 (2010).
37 Wang, K.- R., Guo, D.- S., Jiang, B.- P., Sun, Z.- H. & Liu, Y. Molecular Aggregation Behavior of Perylene-Bridged Bis(β-cyclodextrin) and Its Electronic Interactions upon Selective Binding with Aromatic Guests. *J. Phys. Chem. B* **114,** 101–106 (2010).
38 Jiang, B.- P., Guo, D.- S. & Liu, Y. Reversible and Selective Sensing of Aniline Vapor by Perylene-Bridged Bis(cyclodextrins) Assembly. *J. Org. Chem.* **76,** 6101–6107 (2011).
39 Rekharsky, M. V. & Inoue, Y. Complexation Thermodynamics of Cyclodextrins. *Chem. Rev.* **98,** 1875–1917 (1998).
40 Yamauchi, K., Miyawaki, A., Takashima, Y., Yamaguchi, H. & Harada, A. Switching from altro-α-Cyclodextrin Dimer to pseudo[1]Rotaxane Dimer through Tumbling. *Org. Lett.* **12,** 1284–1286 (2010).
41 Yamauchi, K., Miyawaki, A., Takashima, Y., Yamaguchi, H. & Harada, A. A Molecular Reel: Shuttling of a Rotor by Tumbling of a Macrocycle. *J. Org. Chem.* **75,** 1040–1046 (2010).
42 Fujita, K., Ohta, K., Ikegami, Y., Shimada, H., Tahara, T., Nogami, Y., Koga, T., Saito, K. & Nakajima, T. General method for preparing altrosides from 2,3-manno-epoxides and its application to synthesis of alternative β-cyclodextrin with an altroside as the constituent of macrocyclic structure. *Tetrahedron Lett.* **35,** 9577–9580 (1994).
43 Nogami, Y., Nasu, K., Koga, T., Ohta, K., Fujita, K., Immel, S., Lindner, H. J., Schmitt, G. E. & Lichtenthaler, F. W. Molecular modeling of saccharides. 15. Synthesis, structure, and conformational features of α-cycloaltrin: a cyclo-oligosaccharide with alternating 4C1 1C4 pyranoid chairs. *Angew. Chem. Int. Ed. Engl.* **36,** 1899–1902 (1997).
44 Lichtenthaler, F. W. & Mondel, S. Manno- and altro-Sucrose, and some amino-analogs. *Carbohydr. Res.* **303,** 293–302 (1997).
45 Fujita, K., Chen, W.- H., Yuan, D.- Q., Nogami, Y., Koga, T., Fujioka, T., Mihashi, K., Immel, S. & Lichtenthaler, F. W. Guest-induced conformational change in a flexible host: mono-altro-β-cyclodextrin. *Tetrahedron: Asymmetry* **10,** 1689–1696 (1999).
46 Chen, W. H., Fukudome, M., Yuan, D. Q., Fujioka, T., Mihashi, K. & Fujita, K. Restriction of guest rotation based on the distortion of a cyclodextrin cavity. *Chem. Commun.* 541–542 (2000).
47 Liu, Y., Ke, C.- F., Zhadng, H.- Y., Cui, J. & Ding, F. Complexation-Induced Transition of Nanorod to Network Aggregates: Alternate Porphyrin and Cyclodextrin Arrays. *J. Am. Chem. Soc.* **130,** 600–605 (2008).
48 Zhang, B. & Breslow, R. Enthalpic domination of the chelate effect in cyclodextrin dimmers. *J. Am. Chem. Soc.* **115,** 9353–9354 (1993).
49 Briggner, L.- E., Ni, X.- R., Tempesti, F. & Wadsö, I. Microcalorimetric titration of β-cyclodextrin with adamantane-1-carboxylate. *Thermochim. Acta* **109,** 139–143 (1986).
50 Eftink, M. R., Andy, M. L., Byström, K., Perlmutter, H. D. & Kristol, D. S. Cyclodextrin inclusion complexes: studies of the variation in the size of alicyclic guests. *J. Am. Chem. Soc.* **111,** 6765–6772 (1989).
51 Weickenmeter, M. & Wenz, G. Cyclodextrin side chain polyesters. Synthesis and inclusion of adamantane derivatives. *Macromol. Rapid Commun.* **17,** 731–736 (1996).
52 Godínez, L. A., Schwartz, L., Criss, C. M. & Kaifer, A. E. Thermodynamic Studies on the Cyclodextrin Complexation of Aromatic and Aliphatic Guests in Water and Water-Urea Mixtures. Experimental Evidence for the Interaction of Urea with Arene Surfaces. *J. Phys. Chem. B.* **101,** 3376–3380 (1997).

Supplementary Information accompanies the paper on Polymer Journal website (http://www.nature.com/pj)